
Trapping of peptide-based surrogates in an artificially created channel of cytochrome *c* peroxidase

ANNA-MARIA A. HAYS,¹ HARRY B. GRAY,² AND DAVID B. GOODIN¹

¹Department of Molecular Biology, The Scripps Research Institute, La Jolla, California 92037, USA

²Beckman Institute, California Institute of Technology, Pasadena, California 91125, USA

(RECEIVED August 14, 2002; FINAL REVISION November 14, 2002; ACCEPTED November 15, 2002)

Abstract

As recently described, the deliberate removal of the proposed electron transfer pathway from cytochrome *c* peroxidase resulted in the formation of an extended ligand-binding channel. The engineered channel formed a template for the removed peptide segment, suggesting that synthetic surrogates might be introduced to replace the native electron transfer pathway. This approach could be united with the recent development of sensitizer-linked substrates to initiate and study electron transfer, allowing access to unresolved issues about redox mechanism of the enzyme. Here, we present the design, synthesis, and screening of a peptide library containing natural and unnatural amino acids to identify the structural determinants for binding this channel mutant. Only one peptide, (benzimidazole-propionic acid)-Gly-Ala-Ala, appeared to interact, and gave evidence for both reversible and kinetically trapped binding, suggesting multiple conformations for the channel protein. Notably, this peptide was the most analogous to the removed electron transfer sequence, supporting the use of a cavity-template strategy for design of specific sensitizer-linked substrates as replacements for the native electron transfer pathway.

Keywords: Heme enzyme; protein engineering; protein cavities; cavity complementation; chemical rescue; electron transfer pathway; sensitizer-linked substrates

A number of questions about the function of heme enzymes and electron transfer (ET) in general could be addressed in a novel approach by introducing artificial ET pathways into the context of a native enzyme. Cytochrome *c* peroxidase (CCP) forms an ideal scaffold for such studies because it is well characterized and contains a defined structural element

that has been proposed to function as an ET pathway, yet the role of this proposed pathway remains controversial. CCP catalyzes the oxidation of two equivalents of cytochrome *c* (cyt *c*) with the concomitant reduction of H₂O₂ to water (Yonetani 1976). H₂O₂ reacts with the enzyme to form an oxidized intermediate, Compound I, containing the ferryl (Fe⁺⁴=O) heme (Yonetani 1976) and a radical on Trp-191 (Erman et al. 1989; Sivaraja et al. 1989; Houseman et al. 1993; Huyett et al. 1995); in turn, this intermediate is reduced via ET from cyt *c*. Based on a crystal structure of the CCP-cyt *c* complex (Pelletier and Kraut 1992), residues W191-G192-A193-A194 of CCP were proposed to provide an efficient sigma-bond tunneling pathway (Beratan et al. 1992) between the heme of cyt *c* and the Trp-191 radical center of CCP. This proposal has been supported by studies indicating that efficient ET from cyt *c* requires the presence of the Trp-191 radical (Millett et al. 1995; Wang et al. 1996; Mei et al. 1999; Hirst et al. 2001a). However, other studies have indicated multiple binding sites for cyt *c* on CCP, and thus it remains unresolved whether multiple or

Reprint requests to: David B. Goodin, Department of Molecular Biology, MB8, The Scripps Research Institute, 10550 N. Torrey Pines Road, La Jolla, CA 92037, USA; e-mail: dbg@scripps.edu; fax: (858) 784-2857.

Abbreviations: CCP, cytochrome *c* peroxidase; SLS, sensitizer-linked substrate; cyt *c*, cytochrome *c*; ET, electron transfer; P450cam, cytochrome P450cam; HBTU, 2-(1H-benzotriazol-1-yl)-1,1,3,3-tetramethyluronium hexafluorophosphate; HOBt, N-hydroxybenzotriazole; Fmoc, 9-fluorenylmethoxycarbonyl; Dde, 4,4-dimethyl-2,6-dioxocyclohex-1-ylidene-ethane; DMF, *N,N*-dimethylformamide; TEA, triethylamine; TFA, trifluoroacetic acid; TIS, tri-isopropylsilane; BTP, bistrispropane; CA, citric acid; ITC, isothermal titration calorimetry; GuHCl, guanidine hydrochloride; Ru-C₁₁-Im, Ru-C₉-EB, Ru-F₈bp-Im, Ru-F₉bp (Ru = [Ru^{II}(bpy)₃]²⁺, C₁₁ = —(CH₂)₁₁—, C₉ = —(CH₂)₉—, Im = imidazole, EB = ethylbenzene, F₈bp = 4,4'-octafluorobiphenyl, F₉bp = 4,4'-nonafluorobiphenyl).

Article and publication are at <http://www.proteinscience.org/cgi/doi/10.1110/ps.0228403>.

heterogeneous ET pathways are used in CCP (Miller et al. 1996; Erman et al. 1997; Nocek et al. 1997; Wang and Pielak 1999; Leesch et al. 2000; Nocek et al. 2000). The electrostatic environment surrounding the Trp radical has been proposed to strongly influence the stability of the radical (Fitzgerald et al. 1995; Jensen et al. 1998; Bonagura et al. 1999; Wirstam et al. 1999). In addition, the oxidation of the enzyme to Compound I induces significant changes in the disorder of the proposed ET chain, suggesting that gated ET may play an important role in this enzyme (T. Poulos, pers. comm.). Thus, the ET pathway may respond in a functionally specialized manner in the context of the surrounding protein, yet the exact nature of these roles has not been firmly established. For these reasons, it would be of considerable interest to replace the native ET pathway with a set of artificial structures that could be modified systematically.

Sensitizer-linked substrates (SLS) have recently been developed as a novel tool for engineering molecular recognition and function in redox active enzymes. For example, SLS probes containing a Ru-diimine sensitizer, linker, and substrate analog, have been designed to bind with high affinity and specificity to P450cam such that the substrate analog portion of the SLS occupies the enzyme active site, the sensitizer is at the protein surface, and the linker is threaded through a channel in the protein between the two sites (Dmochowski et al. 1999, 2000, 2001; Wilker et al. 1999; Dunn et al. 2001). Photoexcitation of SLS probes containing Ru-sensitizers can be utilized to initiate ET through the probe to the active site, driving rapid oxidation or reduction of the buried heme. This approach may thus provide a new method to prepare unstable redox intermediates and follow their subsequent reactions (Dmochowski et al. 1999; Wilker et al. 1999; Dunn et al. 2001). More recently, SLS probes containing dansyl fluorophores have been designed that are quenched upon binding P450cam by Förster energy transfer to the heme (Dunn et al. 2002). Fluorescence is restored when the probe is displaced by camphor, demonstrating that these probes may be useful in identifying substrate-based inhibitors. Consequently, SLS probes have great potential as a new tool for studying the redox chemistry of metalloproteins or as sensing elements for protein detection, molecular recognition events, and inhibitor discovery.

To date, these probes have been introduced into preexisting protein channels, but recent work suggests that it may be possible to explore an approach in which both the protein and the SLS are designed to be complementary. Several studies have shown that small molecule binding sites can be introduced into a protein by cavity engineering (Toney and Kirsch 1989; Vandekamp et al. 1990; Eriksson et al. 1992; Denblauwen et al. 1993; Barrick 1994; Fitzgerald et al. 1994, 1995, 1996; McRee et al. 1994; Wilks et al. 1995; Goodin 1996; Newmyer and Ortiz de Montellano 1996;

Musah and Goodin 1997, 1999; Musah et al. 1997, 2002; Hays et al. 1998; Hirst and Goodin 2000; Hirst et al. 2001a, 2001b). Often, it appears that the energetic penalty associated with repacking the protein around an engineered cavity exceeds that of leaving the cavity intact (Morton and Matthews 1995; Baldwin et al. 1998). Thus, in a surprising number of cases, cavities introduced by mutagenic truncation of side chains do not collapse, but instead leave behind templates capable of binding small molecules that complement the packing, hydrogen bonding, and electrostatic interactions that were removed (McRee et al. 1994; Fitzgerald et al. 1995, 1996; Goodin 1996; Musah and Goodin 1997, 1999; Musah et al. 1997, 2002; Hirst and Goodin 2000; Hirst et al. 2001a, 2001b). We have shown that if the structure of the cavities and their response to ligand binding can be analyzed in detail, it is possible to use multiple design cycles to guide larger scale excavation of targeted segments of a protein structure. Using this approach, the proposed ET pathway was recently removed from CCP, resulting in a completely artificial 15 Å-deep channel extending from the surface of the enzyme to the proximal heme face (Fig. 1) (Rosenfeld et al. 2002). The dimensions of the water-filled channel match those of the removed ET chain fairly accurately, and benzimidazole was observed to bind at the position of the Trp-191 radical side chain. These results suggest that suitably designed synthetic surrogates may bind to the excavated channel and restore electron transfer properties to the enzyme.

In this study, we report our results on the binding behavior of a library of synthetic peptides as candidates for the replacement of the proposed ET pathway. Both side chain and backbone properties were varied to allow identification of the important structural elements. The results indicate binding only for structures that accurately mimic the removed ET pathway. They also suggest that the engineered channel may exist in at least two conformations, and that these species display reversible and kinetically trapped behavior, respectively. These results are discussed in terms of their value in the next stage of designing functional artificial ET pathways in this enzyme.

Results

Design of the peptide library

The structure of the engineered channel mutant (Rosenfeld et al. 2002) provided important observations to guide the design of our initial library. The channel envelops the excised structure very closely, with only minor changes in the surrounding protein forming the walls of the channel (Fig. 1). Thus, the channel should serve as a template for molecules with roughly complementary structure and hydrogen bonding potential. Shown in Figure 2 are the hydrogen bonding interactions between the proposed ET pathway se-

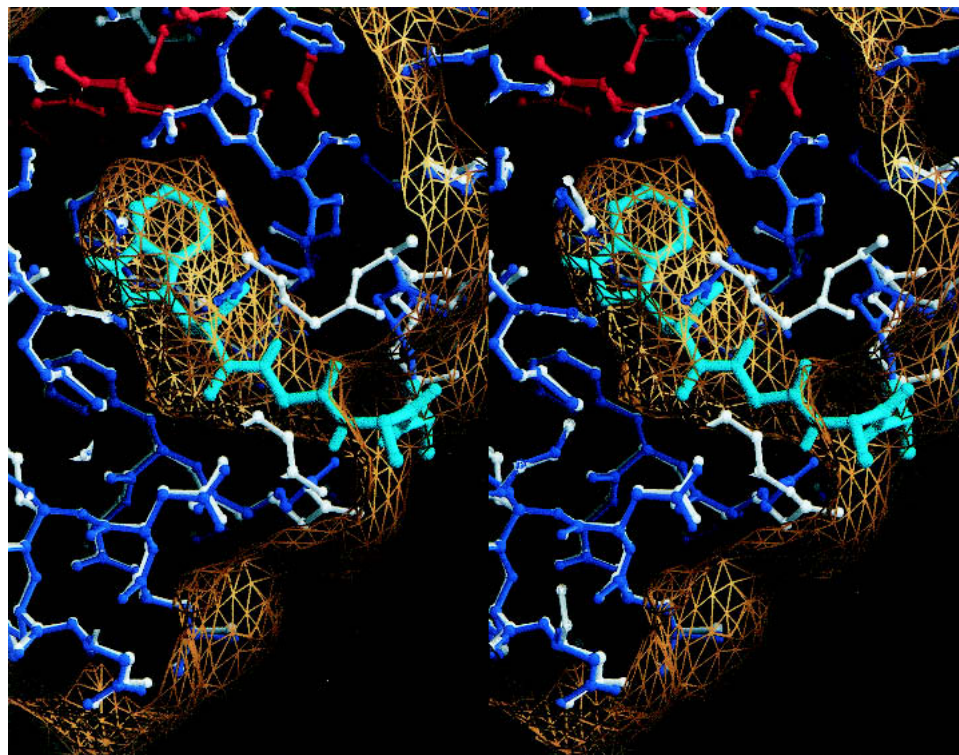


Figure 1. Stereoview of the 1.9-Å crystal structure of the engineered channel mutant (white) superimposed on the structure of wild-type CcP (blue). The proposed ET pathway is highlighted (cyan). The solvent accessible surface of the channel mutant is shown in gold.

quence, Trp-Gly-Ala-Ala, and the surrounding protein as seen in the wild-type enzyme. An important interaction is formed between the indole nitrogen of Trp-191 and Asp-235 (Goodin and McRee 1993; Musah et al. 2002). In turn, the carbonyl oxygen of Trp-191 and the amide groups of Ala-193 and Ala-194 form hydrogen bonds with side chains of nearby residues (Asn-205 and Glu-201). Additional hydrogen bonds are seen between polar groups on the peptide segment and ordered solvent molecules (H₂O-308 and H₂O-310) or are exposed on the surface of the protein. However, the structure of the engineered channel mutant (Rosenfeld et al. 2002) suggested that a direct analog of the removed peptide (Trp-Gly-Ala-Ala) may not constitute an ideal surrogate. The shortened loop of the channel mutant resulted in a rethreading of the protein mainchain across the position occupied by H₂O-308 in the WT structure (see Fig. 1). In addition, the position of this rethreaded segment changed in response to benzimidazole binding within the channel. Accordingly, we considered that the ideal surrogate might require an alternate arrangement of hydrogen bonding interactions compared to those observed with the WT ET chain. A second critical observation was that benzimidazole and other positively charged heterocycles bind in the cavity, but that analogous neutral compounds do not. Benzimidazole was observed to overlay the position of the indole ring of the WT Trp-191 side chain (Rosenfeld et al. 2002). This

specificity for cationic heterocycles is also seen with the W191G cavity, and presumably reflects the electrostatics of the surrounding protein that has evolved to stabilize the

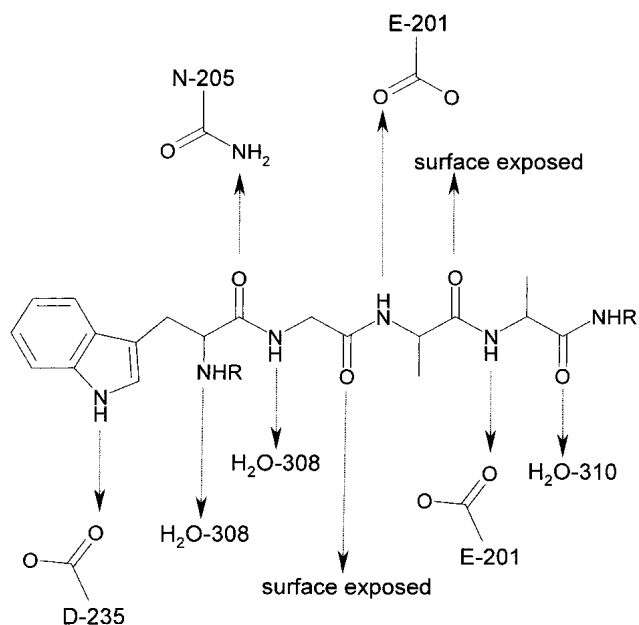


Figure 2. Specific hydrogen bonding interactions observed between the proposed ET peptide of WT CCP and the surrounding protein scaffold.

radical cation form of Trp-191 (Fitzgerald et al. 1994, 1995, 1996; Musah and Goodin 1997; Musah et al. 1997, 2002). The favorable binding enthalpy of heterocyclic cations therefore suggests that these cations might serve as bait for introducing artificial surrogates with a defined specificity for this channel.

To evaluate the effects of alternate hydrogen bonding patterns and the role of the bait residue, a peptide library, shown in Figure 3, was constructed in which both of these features were varied. A number of cationic and neutral groups of the appropriate size were introduced at the bait position, followed by a peptide backbone that contained both natural and unnatural amino acids, including alanine, glycine, β -alanine, and γ -aminobutyric acid. Thus, peptides exhibit the desired shape complementarity while providing variation in the spacing and placement of potential hydrogen bonding groups.

Screening for reversible binding

Two methods were used to screen the peptides (Fig. 3) for behavior consistent with reversible binding to the channel

mutant. Ligand binding to cavities adjacent to the heme can be detected by a small perturbation of the heme Soret band in UV/Vis spectra (Fitzgerald et al. 1994, 1996; Musah and Goodin 1997; Musah et al. 1997, 2002; Rosenfeld et al. 2002). In addition, binding was evaluated by isothermal titration calorimetry (ITC), which measures the binding enthalpy directly independent of spectroscopic changes. To eliminate the known competition by buffer cations and to ensure protonation of the ligands, all binding titrations were performed in 100 mM BTP/CA/4.5 (Musah et al. 2002). As shown in Figure 4, benzimidazole binding to the channel mutant was easily detected by both spectroscopic titration and ITC. However, **17**, consisting of (benzimidazole-propionic acid)-Gly-Ala-Ala, was the only peptide in the library to give indication of reversible binding by UV/Vis and ITC. Most significantly, changing the charged bait residue to a neutral tryptophan while retaining the peptide backbone (**1**) resulted in the loss of binding behavior. Likewise, changing the pattern of hydrogen bonding groups in the peptide while retaining the charged benzimidazole-propionic acid (**19**) also resulted in complete loss of binding. Finally, no bind-

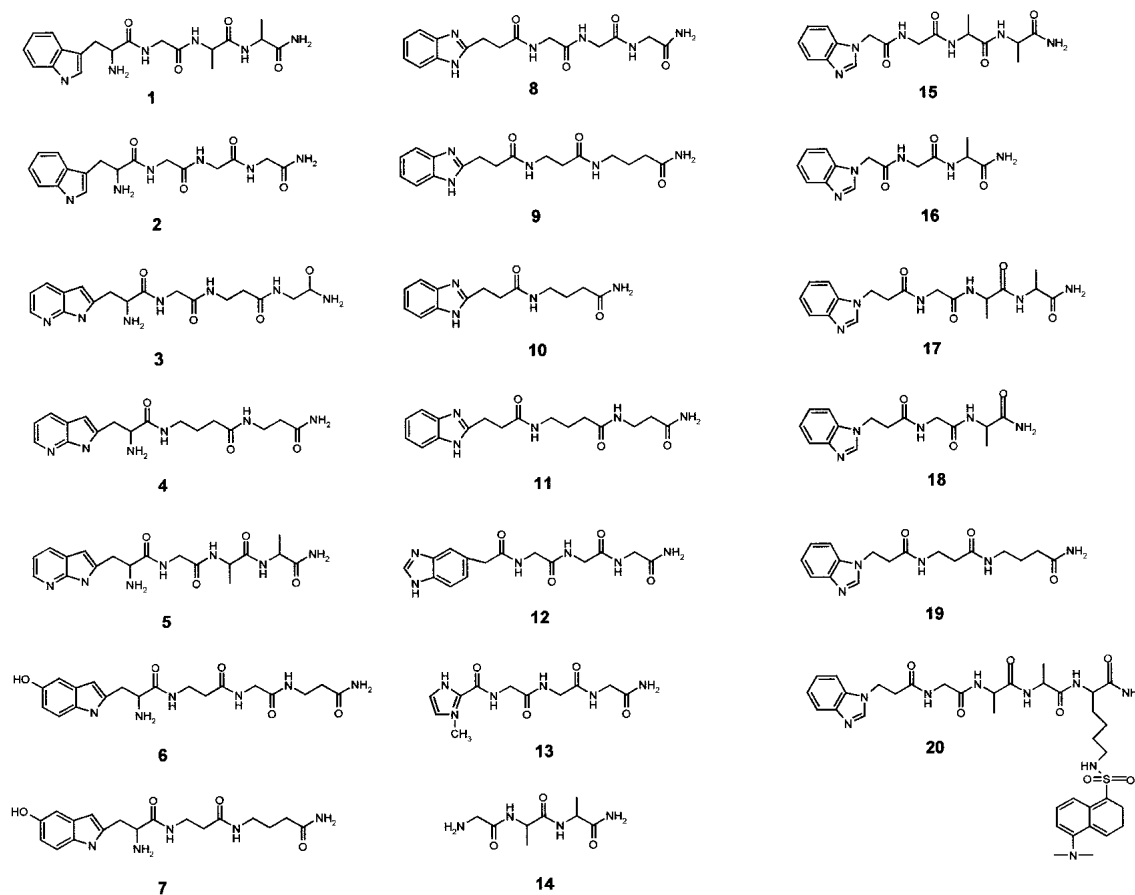


Figure 3. The peptide library used to screen for interactions with the channel mutant of CCP. Peptides were synthesized by solid-phase peptide synthesis (Fmoc chemistry). To maximize all possible hydrogen bonding interactions that could be observed between the peptides and residues lining the channel, the bait residue and peptide linkers were varied.

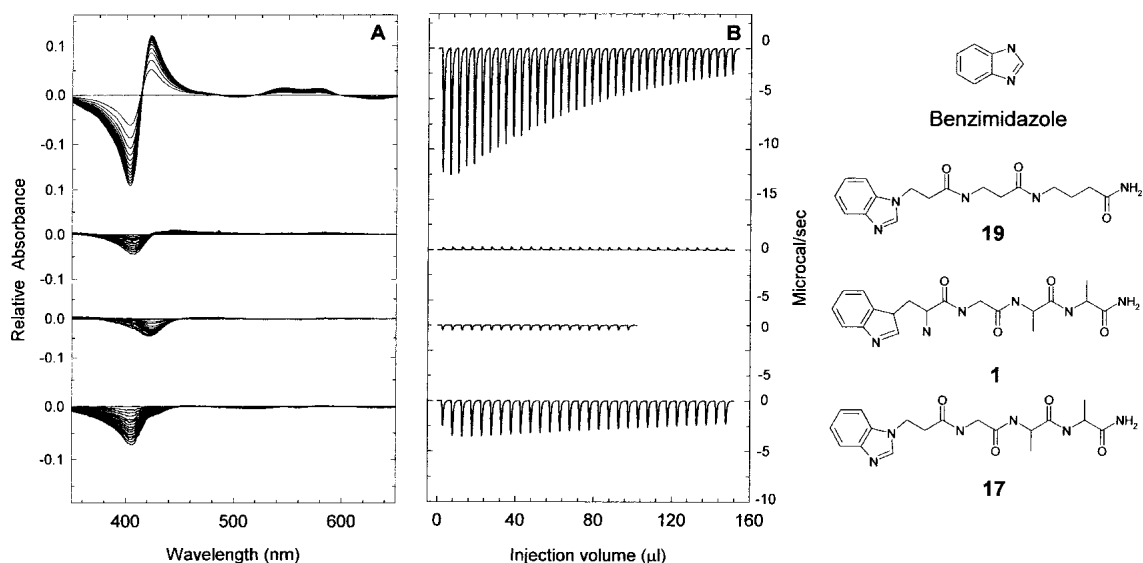


Figure 4. Reversible interaction of peptides with the channel mutant as observed by difference absorption spectroscopy (A) and isothermal titration calorimetry (B). Conditions for UV/Vis binding measurements: 100 mM BTP/CA/4.5, 50 μ M protein, 5 μ L additions of 50 mM peptide, 25°C. Conditions for ITC: 200 mM BTP/CA/4.5, 500 μ M protein, 5 μ L additions of 20 mM peptide.

ing was detected when peptides were titrated into WT CCP (data not shown). Although fits to ITC titrations of **17** gave an approximate K_d of 5 mM, these values are uncertain due to the weak interaction and the correlation between estimated K_d and binding stoichiometry.

Kinetic trapping of peptide surrogates

Trapping experiments were performed to test the possibility that the peptide surrogates may be prevented from reversible entry into the relatively restricted engineered channel. From the crystal structure of the channel mutant, it is clear that the peptides of Figure 3 could not completely enter the channel without some level of dynamic movement of the cavity walls. Attempts to investigate this effect by examination of binding behavior at elevated temperatures proved inconclusive due to protein instability. However, we have obtained evidence for trapping of peptides in the channel mutant after partial denaturation/refolding. For these experiments, we used **20**, a version of **17** labeled with a dansyl fluorophore (Fig. 3). **20** was synthesized by adding a lysine to the N-terminal end of the **17**, followed by addition of the fluorescent dansyl reporter group ($\lambda_{\text{ex}} = 330$ nm, $\lambda_{\text{em}} = 550$ nm) to the amino group of the lysine side chain. To trap the peptides, the protein was first incubated in the presence of guanidine hydrochloride (GuHCl) at a concentration sufficient to cause some disruption of tertiary structure, but well below that resulting in complete denaturation and loss of heme. To determine the ideal GuHCl concentration, the channel mutant was titrated with GuHCl in 200 mM BTP/CA/4.5 at 25°C while monitoring the heme Soret

absorbance. Under these conditions, we determined that 500 mM GuHCl is slightly below the point where a significant change in heme absorbance occurs (data not shown).

For the trapping experiments, the channel mutant (75 μ M) was incubated for 30 min in 500 mM GuHCl, 200 mM BTP/CA/4.5 at 25°C along with a 13-fold excess of **20** (1 mM). Gel filtration in buffer containing **20** but not GuHCl was used to initiate refolding with the removal of GuHCl, followed by a second gel filtration in buffer to remove unbound **20**. Fluorescence spectra of the resulting protein (Fig. 5A) showed that **20** remains trapped by the channel mutant after this treatment. Significantly, no trapping is observed when the order of removal is reversed and peptide is removed before refolding (Fig. 5D). Additionally, we note that the observed emission maximum of **20** is red-shifted by 13 nm when bound to the channel mutant. To demonstrate that the binding of **20** is not dependent on the dansyl group, the trapping experiment was repeated in the presence of **17** at 1 and 10 mM concentrations. The resulting fluorescence spectra (Fig. 5B, 5C, respectively) exhibit a significant loss in signal, thus clearly demonstrating that **17** is able to compete with **20** for the same binding site.

Activity measurements

Finally, we have examined the functional effects of reconstituting **20** into the channel mutant. As expected, the activity of the channel mutant, as measured by the steady-state rate of oxidation of horse heart ferrocyanide *c* by H_2O_2 is reduced to less than 0.1% of the rate observed for WT CCP ($\sim 300 \text{ sec}^{-1}$). The activity of the channel mutant after

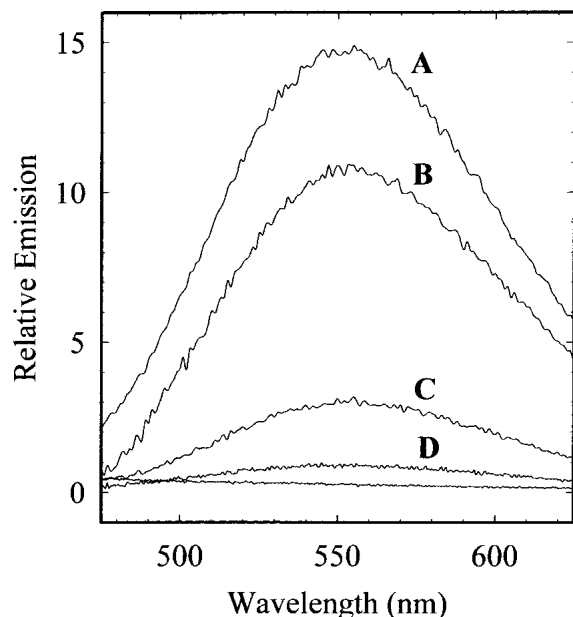


Figure 5. Kinetic trapping of **20** within the channel mutant of CCP. Protein (75 μ M) was incubated in the presence of 500 mM GuHCl and 13-fold excess **20** (1 mM). In **A**, GuHCl was removed prior to removal of the peptide by sequential gel filtration. In **D**, the order of removal was reversed. Fluorescence spectra of the resulting protein shows evidence for trapping of **20** (**A**), but if the peptide is removed prior to refolding, no trapping occurs (**D**). The experiment as performed in **A** was repeated in the presence of either 1 mM or 10 mM **17**. The resulting spectra (**B** and **C**, respectively) demonstrate significantly less trapping of **20**, providing evidence that the two SLS probes are competing for the same binding site.

reconstitution with **20** also remained less than 0.15% of the WT CCP rate. It is noted that we do not at present have an accurate determination of the fractional occupation of the peptide in the protein.

Discussion

Several conclusions can be made about the cavity-template approach for replacing a defined element of protein structure with a synthetic element. The existence of detailed structures for both WT CCP and the channel mutant enabled the design of synthetic surrogate candidates that would preserve interactions observed in the native pathway, while adapting to small changes seen upon its excision. This analysis suggested that the hydrophobic linkers used in previous SLS probes of P450cam would not complement the hydrogen-bonding and electrostatic properties of the engineered channel mutant. Indeed, we have observed no evidence of interaction of the P450 specific SLS probes Ru-C₁₁-Im, Ru-C₉-EB, or Ru-F₈bp-Im (Wilker et al. 1999; Dmochowski et al. 2000, 2001; Dunn et al. 2001, 2002) with the channel mutant (data not shown). Consequently, both natural and unnatural peptides were utilized to permit

comparable flexibility and variation in spacing of possible hydrogen bond donors and acceptors.

In one sense, success would seem to depend strongly on the availability of structural information for both the original and excavated proteins. Clearly, structures were critical in verifying that the cavity template was created without significant rearrangement of the surrounding protein. The unpredictable response of a protein structure to mutagenic variation has made it imperative to combine structural characterization with mutagenesis studies. It thus remains remarkable how often cavity creating mutants result in minimal collapse of the surrounding structure (Toney and Kirsch 1989; Vandekamp et al. 1990; Eriksson et al. 1992; Denblauwen et al. 1993; Barrick 1994; Fitzgerald et al. 1994, 1995, 1996; McRee et al. 1994; Morton and Matthews 1995; Wilks et al. 1995; Goodin 1996; Newmyer and Ortiz de Montellano 1996; Musah and Goodin 1997, 1999; Musah et al. 1997, 2002; Baldwin et al. 1998; Hays et al. 1998; Hirst and Goodin 2000; Hirst et al. 2001a, 2001b). Clearly, cavities are often not as energetically disruptive as mutants that force alternate packing solutions, and lost hydrogen bonds can often be replaced by strategically placed solvent with minimal energetic cost. However, for binding surrogates, these will become very important considerations. Small movements of the cavity walls during excavation could easily offset the 3–5 kcal/mole binding free energy that is likely to result from initial screens for surrogate molecules, suggesting that the template structure must be examined carefully for potentially disruptive changes. In addition, the surrogate must accurately recapture all of the lost hydrogen bonding interactions of the original structure to avoid irretrievable penalties in binding free energy.

In this regard, our results with the CCP channel mutant are quite surprising. The structure of the channel mutant showed that the shortened sequence was rethreaded through an adjacent region, displacing a solvent molecule that contributed a hydrogen bond to the removed mainchain. Although this rethreaded sequence could provide a hydrogen bond to a surrogate peptide in place of the lost solvent molecule, it is unclear if it does so. As this segment was observed to move in response to benzimidazole binding (Rosenfeld et al. 2002), it is also possible that rearrangement of this segment allows solvent to play its native role. It was this alteration that prompted our use of a library of alternate backbone configurations, as it was uncertain if the redesigned channel could regain hydrogen bonding by a completely analogous surrogate. However, it appears that the native template remains the most ideal among those that we have examined at this point. Thus, despite indications from the structure to the contrary, the cavity-template approach appears to provide an efficient method for design of highly specific surrogate ligands.

A number of conclusions may also be inferred about the mode of interaction for the designed peptides with the en-

gineered channel. First, binding affinity appears to require a cationic heterocycle at the position analogous to the Trp-191 cation, and it appears to depend strongly on the arrangement of hydrogen bonding atoms in the peptide backbone. Notably, the only peptide to exhibit clear binding behavior was peptide **17** (and the variant **20**), which accurately reproduces the features found in the native enzyme. This effectively defines a strategy for the design of specific surrogates based on the cavity-template approach used for smaller cavities in this and other enzymes (Vandekamp et al. 1990; Denblauwen et al. 1993; Barrick 1994; Fitzgerald et al. 1994, 1995, 1996; McRee et al. 1994; Wilks et al. 1995; Goodin 1996; Newmyer and Ortiz de Montellano 1996; Musah and Goodin 1997, 1999; Musah et al. 1997, 2002; Hays et al. 1998; Hirst and Goodin 2000; Hirst et al. 2001a, 2001b). Second, this same peptide, **20**, also exhibited behavior consistent with its being kinetically trapped in the protein after partial denaturation/refolding. This behavior is distinct from that exhibited by the W191G mutant, where the cavity is completely buried yet reversibly binds a range of ligands (Fitzgerald et al. 1996; Musah et al. 2002). The results with W191G suggest that the protein undergoes a degree of conformation dynamics that allows transient access of ligands to the buried cavity, while kinetic trapping of the larger peptides in the channel mutant suggests that such states are not thermally accessible. It is possible that peptide entry into the channel would require larger conformational changes, or perhaps sequential multi-step transitions similar to that proposed for acetylcholinesterase (Shen et al. 2001; Lin et al. 2002).

The observation of both reversible binding and kinetic trapping behavior by **17** and **20** deserves comment, as these properties would seem to be mutually inconsistent. Clearly, one explanation is that two sites exist for interaction with the channel mutant, although several observations disfavor this possibility. First, both behaviors appear to be dependent on the cation and backbone arrangement in the peptide that matches the cavity template. Second, the reversible binding behavior is not seen for the WT enzyme, suggesting that it is dependent on the existence of the channel. We note that trapping experiments performed with **20** using the WT enzyme provide some evidence for trapping of the peptide. However, this is not inconsistent with its binding at the channel site, because we have previously found that the best ligands for the W191G cavity are able to displace the Trp-191 side chain from WT CCP and induce a conformational change in the ET pathway segment that mimics our channel mutant (Cao et al. 1998). Thus, although two spatially distinct sites may exist on the channel enzyme that are both specific for **17** and **20**, we favor a model in which the channel itself exists in more than one conformational state, one of which allows reversible binding, and another that presents a thermally inaccessible barrier to ligand entry and exit.

The specific interactions observed between **17** or **20** and the channel mutant appear to be similar to those observed with small peptides binding to the oligopeptide binding protein OppA (Sleigh et al. 1999). These studies have shown that a complete picture of a protein-peptide complex requires not only analysis of the complex, but also solvation changes upon association (Davies et al. 1999; Sleigh et al. 1999). Studies have also shown that ligand binding can be controlled by dynamic processes involving conformational flexibility around the native state (Shen et al. 2001; Lin et al. 2002; Ma et al. 2002). Similar processes have also been studied by X-ray crystallography, in which regions of high thermal factors are indicative of preferred paths for ligand entry from the solvent to the protein core (Carugo and Argos 1998). These preexisting populations are in equilibrium, and therefore guide ligand binding, yet the shape of the binding site can also be influenced by the molecular partner (Fitzgerald et al. 1994; Ma et al. 2002; Musah et al. 2002; Rosenfeld et al. 2002).

In conclusion, we have taken steps to establish host-guest replacement of the proposed ET pathway of CCP by simultaneous design of the ligand and protein binding site. Our study has established the utility of the cavity-template approach for introducing peptides that are structurally analogous to excised structures. Extension of these peptide templates will provide a basis for the design of specific sensitizer-linked substrates to serve as surrogates for the ET pathway, allowing a new approach to study ET events in redox proteins.

Materials and methods

Protein expression and purification

The channel mutant was constructed in the *Escherichia coli* expression plasmid pT7CCP by oligonucleotide site-directed mutagenesis as previously described (Fitzgerald et al. 1994; Rosenfeld et al. 2002). Protein was overexpressed in *E. coli* BL21(DE3), purified, and reconstituted with heme according to previously reported procedures (Fitzgerald et al. 1994). UV-Vis absorption spectra were used to calculate protein concentration based on the molar absorptivity at 412 nm ($\epsilon = 103.6 \text{ mM}^{-1} \text{ cm}^{-1}$), as determined from pyridine hemochromogens (Nicola et al. 1975; Fitzgerald et al. 1994). Purified protein was recrystallized twice from distilled water and stored as a crystal suspension at 77 K.

Peptide and ligand synthesis

Peptides were synthesized manually on Rink Amide resin (Novabiochem) using a standard protocol for HBTU(Novabiochem)/HOBT (Novabiochem)/collidine (Fluka) activation of 9-fluorenyl methoxycarbonyl(Fmoc)-protected amino acid derivatives: Fmoc-Gly-OH, Fmoc-Ala-OH, Fmoc- β -Ala-OH, Fmoc- γ -aminobutyric acid, Fmoc-Trp-OH, Fmoc-Lys(Dde)-OH (Novabiochem). The side chain of Lys was protected with 4,4-dimethyl-2,6-dioxocyclohex-1-ylidene-ethane. The coupling reaction was performed in dimethylformamide (DMF, Aldrich) for 30 min using two- to

threefold excess of amino acid. Fmoc removal was performed with 20% piperidine (Fluka) in DMF. After peptide chain assembly, three- to fourfold excess of ligand was coupled overnight using either collidine or triethylamine (TEA, Sigma) as base, and when applicable dansylated after the Lys side chain was deprotected using 2% hydrazine in DMF. Cleavage from the resin was achieved with 95% trifluoroacetic acid (TFA, Sigma), 2.5% triisopropylsilane (TIS, Fluka), and 2.5% water for 1 h. The resin was removed by filtration and the remaining TFA solution concentrated under nitrogen flow. The peptides were precipitated with diethyl ether and lyophilized from glacial acetic acid. Peptides were further purified by HPLC (Hitachi L-6200A intelligent pump, L-4200 UV-Vis detector) using a preparatory Supelcosil PLC-18 C18 reversed phase column with a flow rate of 4 mL/min with detection at 230 or 320 nm. Solvent A contained 0.1% TFA in water, and solvent B contained 90% acetonitrile (Sigma) and 10% of a 0.1% aqueous TFA solution. Peptides were eluted with a linear gradient from 0 to 50% B over 55 min. Fractions were lyophilized and analyzed by electrospray mass spectrometry (Scripps Center for Mass Spectrometry).

N-methylimidazole-2-carboxylic acid (Wade et al. 1992) and benzimidazole-1-acetic acid (Upadhyay and Srivastava 1994) were synthesized as previously described. Synthesis of N-benzimidazole propionic acid was performed by refluxing equimolar amounts of benzimidazole (Janssen Chimica), bromopropionic acid (Fluka), and a slight excess of TEA in isopropanol (Sigma) for 5 h. The reaction mixture was concentrated and stored overnight at -20°C . Acetonitrile was added and stirred at room temperature for 2 h, and solvent removed on a roto-evaporator. The final product yielded N-benzimidazole propionic acid with a yield of approximately 30%–40%. 2-Benzimidazole propionic acid, 5-benzimidazole carboxylic acid, indole-3-propionic acid, azatryptophan and 5-hydroxy tryptophan were purchased from Sigma-Aldrich or AnaSpec Inc. and used as received.

Binding measurements

Protein was prepared for binding experiments by dissolving crystals in 500 mM Bis-Tris propane/citric acid at pH 4.5 (BTP/CA/4.5) to give a stock solution, and then diluted to give desired protein concentration and ionic strength for individual measurements. Peptide solutions were prepared in the same buffer solution as the protein and concentrations determined by weight or estimated utilizing the extinction coefficients of tryptophan or benzimidazole-2-carboxylic acid (Sinha et al. 1989). Measurements of reversible binding were obtained from the observed perturbation of the heme Soret band or by isothermal titration calorimetry (ITC) as described previously for the W191G cavity mutant (Musah et al. 2002). Kinetic trapping of peptides in the channel was inferred by fluorescence measurements of dansylated peptide analogs using a Spex Fluoromax-3 fluorimeter (Jobin Yvon Inc.). The concentration of dansylated peptide was estimated using the dansyl molar extinction coefficient ($\epsilon = 3400 \text{ M}^{-1}\text{cm}^{-1}$) at 330 nm. Protein samples (75 μM in 200 mM BTP/CA/4.5) were incubated with 500 mM guanidine HCl (GuHCl, Sigma) and 13-fold excess of dansylated peptide (**20**) for 30 min. The sample was then divided in two. For one sample, the GuHCl was removed first, followed by excess peptide using sequential gel filtration columns (Micro-Spin 6, BioRad) run in buffer A (200 mM BTP/CA/4.5 + 1 mM peptide) and buffer B (200 mM BTP/CA/4.5), respectively. For the other sample, the order of removal was reversed. The emission spectra were scanned between 400 to 700 nm in a reduced-volume quartz cuvette (400 μL) with an excitation wavelength of 330 nm at intervals of 0.5 nm with 1-sec integration time at each wavelength.

The bandwidths for both excitation and emission spectra were 2.5 nm. Both emission correction spectra and blank spectra were subtracted from the raw data emission spectra. For the competition assay, the trapping experiment was repeated in the presence of either 1 or 10 mM **17**. Again, first GuHCl was removed, followed by the removal of excess peptide using sequential gel filtration columns.

Activity measurements

The rate of CCP-catalyzed oxidation of reduced horse heart cytochrome *c* (cyt *c*) by H_2O_2 was determined as previously described (Goodin et al. 1987, 1991), except that the concentration of the channel mutant and the channel mutant reconstituted with **20** was increased to 250 nM, due to the relative unreactivity of the mutant toward cyt *c* oxidation. Kinetic determinants were carried out at 22°C in 20 mM TRIS/phosphate (pH 6.45), 25 μM reduced cyt *c*, and 10–120 μM H_2O_2 .

Acknowledgments

We thank Drs. Stefan Vetter, Alycen Nigro, and Laura Hunsicker-Wang as well as Alex Dunn for help and valuable discussions. This work was supported by NIH Grants GM41049 and GM48495 (to D.B.G. and H.B.G.), and NIH NRSA Postdoctoral Fellowship GM20703-03 (to A-M.A.H.).

The publication costs of this article were defrayed in part by payment of page charges. This article must therefore be hereby marked "advertisement" in accordance with 18 USC section 1734 solely to indicate this fact.

References

- Baldwin, E., Baase, W.A., Zhang, X., Feher, V., and Matthews, B.W. 1998. Generation of ligand binding sites in T4 lysozyme by deficiency-creating substitutions. *J. Mol. Biol.* **277**: 467–485.
- Barrick, D. 1994. Replacement of the proximal ligand of sperm whale myoglobin with free imidazole in the mutant His-93 > Gly. *Biochemistry* **33**: 6546–6554.
- Beratan, D.N., Onuchic, J.N., Winkler, J.R., and Gray, H.B. 1992. Electron-tunneling pathways in proteins. *Science* **258**: 1740–1741.
- Bonagura, C.A., Sundaramoorthy, M., Bhaskar, B., and Poulos, T.L. 1999. The effects of an engineered cation site on the structure, activity, and EPR properties of cytochrome *c* peroxidase. *Biochemistry* **38**: 5538–5545.
- Cao, Y., Musah, R.A., Wilcox, S.K., Goodin, D.B., and McRee, D.E. 1998. Protein conformer selection by ligand binding observed with crystallography. *Protein Sci.* **7**: 72–78.
- Carugo, O. and Argos, P. 1998. Accessibility to internal cavities and ligand binding sites monitored by protein crystallographic thermal factors. *Proteins Struct. Funct. Genet.* **31**: 201–213.
- Davies, T.G., Hubbard, R.E., and Tame, J.R. 1999. Relating structure to thermodynamics: The crystal structures and binding affinity of eight OppA-peptide complexes. *Protein Sci.* **8**: 1432–1444.
- Denblauwen, T., Hoitink, C.W.G., Canters, G.W., Han, J., Loehr, T.M., and Sandersloehr, J. 1993. Resonance raman spectroscopy of the azurin His117Gly mutant—Interconversion of type-1 and type-2 copper sites through exogenous ligands. *Biochemistry* **32**: 12455–12464.
- Dmochowski, I.J., Crane, B.R., Wilker, J.J., Winkler, J.R., and Gray, H.B. 1999. Optical detection of cytochrome P450 by sensitizer-linked substrates. *Proc. Natl. Acad. Sci.* **96**: 12987–12990.
- Dmochowski, I.J., Winkler, J.R., and Gray, H.B. 2000. Enantiomeric discrimination of Ru-substrates by cytochrome P450cam. *J. Inorg. Biochem.* **81**: 221–228.
- Dmochowski, I.J., Dunn, A.R., Wilker, J.J., Crane, B.R., Green, M.T., Dawson, J.H., Sligar, S.G., Winkler, J.R., and Gray, H.B. 2002. Sensitizer-linked substrates and ligands: Ruthenium probes of cytochrome P450 structure and mechanism. *Methods Enzymol.* **357**: 120–133.
- Dunn, A.R., Dmochowski, I.J., Bilwes, A.M., Gray, H.B., and Crane, B.R.

2001. Probing the open state of cytochrome P450cam with ruthenium-linker substrates. *Proc. Natl. Acad. Sci.* **98**: 12420–12425.
- Dunn, A.R., Hays, A.-M.A., Chiu, R., Winkler, J.R., Stout, C.D., Goodin, D.B., and Gray, H.B. 2002. Fluorescent probes for cytochrome P450 structural characterization and inhibitor screening. *J. Am. Chem. Soc.* **124**: 10254–10255.
- Eriksson, A.E., Baase, W.A., Wozniak, J.A., and Matthews, B.W. 1992. A cavity-containing mutant of T4 lysozyme is stabilized by buried benzene. *Nature* **355**: 371–373.
- Erman, J.E., Vitello, L.B., Mauro, J.M., and Kraut, J. 1989. Detection of an oxyferryl porphyrin π -cation-radical intermediate in the reaction between hydrogen peroxide and a mutant yeast cytochrome *c* peroxidase. Evidence for tryptophan-191 involvement in the radical site of compound I. *Biochemistry* **28**: 7992–7995.
- Erman, J.E., Kresheck, G.C., Vitello, L.B., and Miller, M.A. 1997. Cytochrome *c*/cytochrome *c* peroxidase complex: Effect of binding-site mutations on the thermodynamics of complex formation. *Biochemistry* **36**: 4054–4060.
- Fitzgerald, M.M., Churchill, M.J., McRee, D.E., and Goodin, D.B. 1994. Small molecule binding to an artificially created cavity at the active site of cytochrome *c* peroxidase. *Biochemistry* **33**: 3807–3818.
- Fitzgerald, M.M., Trester, M.L., Jensen, G.M., McRee, D.E., and Goodin, D.B. 1995. The role of aspartate-235 in the binding of cations to an artificial cavity at the radical site of cytochrome *c* peroxidase. *Protein Sci.* **4**: 1844–1850.
- Fitzgerald, M.M., Musah, R.A., McRee, D.E., and Goodin, D.B. 1996. A ligand-gated, hinged loop rearrangement opens a channel to a buried artificial protein cavity. *Nat. Struct. Biol.* **3**: 626–631.
- Goodin, D.B. 1996. When an amide is more like histidine than imidazole: The role of axial ligands in heme catalysis. *J. Biol. Inorg. Chem.* **1**: 360–363.
- Goodin, D.B. and McRee, D.E. 1993. The Asp-His-Fe triad of cytochrome-*c* peroxidase controls the reduction potential, electronic structure, and coupling of the tryptophan free radical to the heme. *Biochemistry* **32**: 3313–3324.
- Goodin, D.B., Mauk, A.G., and Smith, M. 1987. The peroxide complex of yeast cytochrome *c* peroxidase contains two distinct radical species, neither of which resides at methionine 172 or tryptophan 51. *J. Biol. Chem.* **262**: 7719–7724.
- Goodin, D.B., Davidson, M.G., Roe, J.A., Mauk, A.G., and Smith, M. 1991. Amino acid substitutions at tryptophan-51 of cytochrome-*c* peroxidase—Effects on coordination, species preference for cytochrome-*c*, and electron transfer. *Biochemistry* **30**: 4953–4962.
- Hays, A.M., Vassiliev, I.R., Golbeck, J.H., and Debus, R. J. 1998. Role of D1-His190 in proton-coupled electron transfer reactions in photosystem II: A chemical complementation study. *Biochemistry* **37**: 11352–11365.
- Hirst, J. and Goodin, D.B. 2000. Unusual oxidative chemistry of N^w-hydroxy-arginine and N-hydroxyguanidine catalyzed at an engineered cavity in a heme peroxidase. *J. Biol. Chem.* **275**: 8582–8591.
- Hirst, J., Wilcox, S.K., Ai, J., Moëgne-Loccoz, P., Loehr, T.M., and Goodin, D.B. 2001a. Replacement of the axial histidine ligand with imidazole in cytochrome *c* peroxidase. 2. Effects on heme coordination and function. *Biochemistry* **40**: 1274–1283.
- Hirst, J., Wilcox, S.K., Williams, P.A., Blankenship, J., McRee, D.E., and Goodin, D.B. 2001b. Replacement of the axial histidine ligand with imidazole in cytochrome *c* peroxidase. 1. Effects on structure. *Biochemistry* **40**: 1265–1273.
- Houseman, A.L.P., Doan, P.E., Goodin, D.B., and Hoffman, B.M. 1993. Comprehensive explanation of the anomalous EPR spectra of wild-type and mutant cytochrome-*c* peroxidase compound-ES. *Biochemistry* **32**: 4430–4443.
- Huyett, J.E., Doan, P.E., Gurbiel, R., Houseman, A.L.P., Sivaraja, M., Goodin, D.B., and Hoffman, B.M. 1995. Compound ES of cytochrome *c* peroxidase contains a Trp p-cation radical: Characterization by CW and pulsed Q-band ENDOR spectroscopy. *J. Am. Chem. Soc.* **117**: 9033–9041.
- Jensen, G.M., Bunte, S.W., Warshel, A., and Goodin, D.B. 1998. Energetics of cation radical formation at the proximal active site tryptophan of cytochrome *c* peroxidase and ascorbate peroxidase. *J. Phys. Chem. B* **102**: 8221–8228.
- Leesch, V.W., Bujons, J., Mauk, A.G., and Hoffman, B.M. 2000. Cytochrome *c* peroxidase-cytochrome *c* complex: Locating the second binding domain on cytochrome *c* peroxidase with site-directed mutagenesis. *Biochemistry* **39**: 10132–10139.
- Lin, J.-H., Perryman, A.L., Schames, J.R., and McCammon, J.A. 2002. Computational drug design accommodating receptor flexibility: The relaxed complex scheme. *J. Am. Chem. Soc.* **124**: 5632–5633.
- Ma, B., Shatsky, M., Wolfson, H.J., and Nussinov, R. 2002. Multiple diverse ligands binding at a single protein site: A matter of pre-existing populations. *Protein Sci.* **11**: 184–197.
- McRee, D.E., Jensen, G.M., Fitzgerald, M.M., Siegel, H.A., and Goodin, D.B. 1994. Construction of a bisaqueo heme enzyme and binding by exogenous ligands. *Proc. Natl. Acad. Sci.* **91**: 12847–12851.
- Mei, H., Wang, K., Peffer, N., Weatherly, G., Cohen, D.S., Miller, M., Pielak, G., Durham, B., and Millett, F. 1999. Role of configurational gating in intracomplex electron transfer from cytochrome *c* to the radical cation in cytochrome *c* peroxidase. *Biochemistry* **38**: 6846–6854.
- Miller, M.A., Geren, L., Han, G.W., Saunders, A., Beasley, J., Pielak, G.J., Durham, B., Millett, F., and Kraut, J. 1996. Identifying the physiological electron transfer site of cytochrome *c* peroxidase by structure-based engineering. *Biochemistry* **35**: 667–673.
- Millett, F., Miller, M.A., Geren, L., and Durham, B. 1995. Electron transfer between cytochrome *c* and cytochrome *c* peroxidase [review]. *J. Bioenerg. Biomembr.* **27**: 341–351.
- Morton, A. and Matthews, B.W. 1995. Specificity of ligand binding in a buried nonpolar cavity of T4 lysozyme: Linkage of dynamics and structural plasticity. *Biochemistry* **34**: 8576–8588.
- Musah, R.A. and Goodin, D.B. 1997. Introduction of novel substrate oxidation into a heme peroxidase by cavity complementation: Oxidation of 2-aminothiazole and covalent modification of the enzyme. *Biochemistry* **36**: 11665–11674.
- . 1999. Introduction of novel substrate oxidation into cytochrome *c* peroxidase by cavity complementation: Oxidation of 2-aminothiazole and covalent modification of the enzyme. *Chemtracts* **12**: 79–86.
- Musah, R.A., Jensen, G.M., Rosenfeld, R.J., Bunte, S.W., McRee, D.E., and Goodin, D.B. 1997. Variation in strength of a CH to O hydrogen bond in an artificial cavity. *J. Am. Chem. Soc.* **119**: 9083–9084.
- Musah, R.A., Jensen, G.M., Bunte, S.W., Rosenfeld, R.J., and Goodin, D.B. 2002. Artificial protein cavities as specific ligand-binding templates: Characterization of an engineered heterocyclic cation binding site that preserves the evolved specificity of the parent protein. *J. Mol. Biol.* **315**: 845–857.
- Newmyer, S.L. and Ortiz de Montellano, P.R. 1996. Rescue of the catalytic activity of an H42A mutant of horseradish peroxidase by exogenous imidazoles. *J. Biol. Chem.* **271**: 14891–14896.
- Nicola, N.A., Minasian, E., Appleby, C.A., and Leach, S.J. 1975. *Biochemistry* **14**: 5141.
- Nocek, J.M., Zhou, J.S., and Hoffman, B.M. 1997. Quenching as a four-dimensional experiment: Application to the multi-domain binding of cytochrome *c* by cytochrome *c* peroxidase. *J. Electroanal. Chem.* **438**: 55–60.
- Nocek, J.M., Leesch, V.W., Zhou, J.S., Jiang, M., and Hoffman, B.M. 2000. Multi-domain binding of cytochrome *c* peroxidase by cytochrome *c*: Thermodynamic vs. microscopic binding constants. *Isr. J. Chem.* **40**: 35–46.
- Pelletier, H. and Kraut, J. 1992. Crystal structure of a complex between electron transfer partners, cytochrome-*c* peroxidase and cytochrome-*c*. *Science* **258**: 1748–1755.
- Rosenfeld, R.J., Hays, A.-M.A., Musah, R.A., and Goodin, D.B. 2002. Excision of a proposed electron transfer pathway in cytochrome *c* peroxidase and its replacement by a ligand-binding channel. *Protein Sci.* **11**: 1251–1259.
- Shen, T.Y., Tai, K., and McCammon, J.A. 2001. Statistical analysis of the fractal gating motions of the enzyme acetylcholinesterase. *Phys. Rev. E Stat. Nonlinear Soft Matter Phys.* **63**: 0419021–0419026.
- Sinha, H.K., Dogra, S.K., and Sneh K. 1989. Environmental effects on the absorption and fluorescence spectral characteristics of benzimidazole-2-carboxylic acid. *Bull. Chem. Soc. Jpn.* **62**: 2668–2675.
- Sivaraja, M., Goodin, D.B., Smith, M., and Hoffman, B.M. 1989. Identification by ENDOR of Trp191 as the free-radical site in cytochrome *c* peroxidase compound ES. *Science* **245**: 738–740.
- Sleigh, S.H., Seavers, P.R., Wilkinson, A.J., Ladbury, J.E., and Tame, J.R. 1999. Crystallographic and calorimetric analysis of peptide binding to OppA protein. *J. Mol. Biol.* **291**: 393–415.
- Toney, M.D. and Kirsch, J.F. 1989. Direct bronsted analysis of the restoration of activity to a mutant enzyme by exogenous amines. *Science* **243**: 1485–1488.
- Upadhyay, R.K. and Srivastava, S.D. 1994. New heterocycles: Synthesis and biological evaluation. *Indian J. Heterocyclic Chem.* **4**: 121–124.
- Vandekamp, M., Floris, R., Hali, F.C., and Canters, G.W. 1990. Site-directed mutagenesis reveals that the hydrophobic patch of asurin mediates electron transfer. *J. Am. Chem. Soc.* **112**: 907–908.
- Wade, W.S., Mrksich, M., and Dervan, P.B. 1992. Design of peptides that bind in the minor groove of DNA at 5'-(A,T)G(A,T)C(A,T)-3' sequences by a dimeric side-by-side motif. *J. Am. Chem. Soc.* **114**: 8783–8794.
- Wang, K., Mei, H., Geren, L., Miller, M.A., Saunders, A., Wang, X., Pielak,

- G.J., Durham, B., and Millett, F. 1996. Design of a ruthenium-cytochrome *c* derivative to measure electron transfer to the radical cation and oxyferryl heme in cytochrome *c* peroxidase. *Biochemistry* **35**: 15107–15119.
- Wang, X. and Pielak, G.J. 1999. Equilibrium thermodynamics of a physiologically-relevant heme–protein complex. *Biochemistry* **38**: 16876–16881.
- Wilker, J.J., Dmochowski, I.J., Dawson, J.H., Winkler, J.R., and Gray, H.B. 1999. Substrates for rapid delivery of electrons and holes to buried active sites in proteins. *Angew. Chem.* **38**: 90–92.
- Wilks, A., Sun, J., Loehr, T.M., and Ortiz de Montellano, P.R. 1995. Heme oxygenase His25Ala mutant: Replacement of the proximal histidine iron ligand by exogenous bases restores catalytic activity. *J. Am. Chem. Soc.* **117**: 2925–2926.
- Wirstam, M., Blomberg, M.R.A., and Siegbahn, P.E.M. 1999. Reaction mechanism of compound I formation in heme peroxidases: A density functional theory study. *J. Am. Chem. Soc.* **121**: 10178–10185.
- Yonetani, T. 1976. *Cytochrome c peroxidase*. Academic Press, New York.